Biochemical and Biophysical Research Communications xxx (2009) xxx–xxx

Contents lists available at ScienceDirect

Biochemical and Biophysical Research Communications

journal homepage: www.elsevier.com/locate/ybbrc

Kinetics of lipid-membrane binding and conformational change of L-BABP

Vanesa Galassi [a,1], Verónica Nolan [a,1,2], Marcos Ariel Villarreal [a], Massimiliano Perduca [b], Hugo L. Monaco [b], Guillermo G. Montich [a,*]

[a] Centro de Investigaciones en Química Biológica de Córdoba (CIQUIBIC, UNC-CONICET), Departamento de Química Biológica, Facultad de Ciencias Químicas, Universidad Nacional de Córdoba, Haya de la Torre y Medina Allende, Ciudad Universitaria, X5000HUA Córdoba, Argentina
[b] Laboratorio di Biocristallografia, Dipartimento Scientifico e Tecnologico, Università di Verona, Italy

ARTICLE INFO

Article history:
Received 16 March 2009
Available online xxxx

Keywords:
Protein binding to lipid membrane
Protein unfolding
Kinetics
L-BABP
Fluorescence
Stopped-flow

ABSTRACT

We designed an experimental approach to differentiate the kinetics of protein binding to a lipid membrane from the kinetics of the associated conformational change in the protein. We measured the fluorescence intensity of the single Trp6 in chicken liver bile acid-binding protein (L-BABP) as a function of time after mixing the protein with lipid membranes. We mixed the protein with pure lipid membranes, with lipid membranes in the presence of a soluble quencher, and with lipid membranes containing a fluorescence quencher attached to the lipid polar head group. We fitted simultaneously the experimental curves to a three-state kinetic model. We conclude that in a first step, the binding of L-BABP to the interfacial region of the anionic lipid polar head groups occurred simultaneously with a conformational change to the partly unfolded state. In a second slower step, Trp6 buried within the polar head group region, releasing contacts with the aqueous phase.

Introduction

The binding of proteins to the lipid membrane interface is generally coupled to conformational changes. The presence of strong electric fields, changes in water activity, and changes in dielectric constant in the interface, as compared with the bulk solution, can stabilize particular conformations and shift the equilibrium to the membrane-bound state [1]. Bile acid-binding protein from avian liver (L-BABP) is an excellent system to study the coupling between binding and conformational changes in the membrane environment. We found that L-BABP binds to anionic lipid membranes by electrostatic forces and acquires a partly unfolded conformation in the interface [2]. We also found that a pre-molten globule and a molten globule exist in solution and can be populated at low pH [3]. Because a partly unfolded state is observed both in solution and bound to the membrane, two possible paths could explain the coupled process of binding-conformational change. One is that the native protein binds to the lipid membrane and then acquires a partly unfolded state. On the other side, it can be proposed that the unfolded state in solution binds to the interface and the equilibrium is shifted to a partly unfolded, bound state. To study these possibilities, we designed an experimental set-up to distinguish the kinetics of membrane binding from the kinetics of conformational change. We measured the changes in the fluorescence emission of the single Trp6 in stopped-flow experiments after mixing L-BABP with lipid membranes. We used three different experimental arrangements in which the emission intensity is differentially sensitive to the binding and unfolding process. Together with an appropriate curve fitting procedure, this approach proved to be suitable to discriminate between these two processes. Our results show that the conformational change occurred in the interfacial region, simultaneously with the binding, followed by further partial penetration into the polar head group region.

Materials and methods

Materials. L-BABP was purified according to Scapin et al. [4] and stored in 2 mM phosphate buffer, pH 7.3, at −70 °C. Synthetic 1-palmitoyl-2-oleoyl-sn-glycero-3-[phospho-rac-(1-glycerol)] (POPG), 1-palmitoyl-2-oleoyl-sn-glycero-3-phosphocholine (POPC), and L-α-phosphatidylethanolamine-N-(4-nitrobenzo-2-oxa-1,3-diazole) as the ammonium salt (NBD-PE) purified from egg yolk, were obtained from Avanti Polar Lipids (Alabaster, AL). Polycarbonate membranes of 100 nm pore diameter used to extrude the vesicles were from Whatman (Schleicher & Schuel).

Large unilamellar vesicles (LUVs) preparation. Pure POPG and POPC or their mixtures with 5% NBD-PE were dissolved in

* Corresponding author. Fax: +54 351 4334074.
E-mail address: gmontich@mail.fcq.unc.edu.ar (G.G. Montich).
[1] These authors equally contributed to this work.
[2] Present address: Biofísica-Química, Cátedra de Química Biológica, Departmento de Química, Facultad de Ciencias Exactas, Físicas y Naturales, Universidad Nacional de Córdoba, Córdoba, Argentina.

0006-291X/$ - see front matter © 2009 Elsevier Inc. All rights reserved.
doi:10.1016/j.bbrc.2009.03.103

chloroform:methanol 2:1 solution and dried as a thin film in a glass tube. The film was hydrated and re-suspended with 10 mM NaCl solution. LUVs were prepared by freeze–thaw and extrusion in a device from Avestin (Ottawa, Canada). Five cycles of freeze and thaw were done placing the sample for 5 min in a bath with liquid air and 5 min in a water bath at 60 °C. The extrusion step was done at 25 °C, through two stacked 0.1 μm polycarbonate membranes [5]. The method produced vesicles with a mean diameter of 110 nm both for POPG and POPC, according to dynamic light scattering measurements.

Sample preparation. All experiments were carried out at 26 °C. NaCl concentration was 10 mM throughout all the experiments. The concentration of protein was 20 μM for the kinetic experiments, and 10 μM for the measurement of steady-state spectra. The concentration of lipid was 2 mM for the kinetic measurements, and 1 mM for the measurement of steady-state spectra. The concentration of acrylamide in the kinetic experiments was 0.545 M.

Measurement of fluorescence spectra. Steady-state fluorescence spectra were obtained in a Fluoromax 3P spectrofluorometer from Horiba Jobin Yvon (Edison NJ, USA), using a 3 mm optical path length cell, an excitation wavelength of 295 nm. Slits in the excitation and emission channel were 1 and 3 nm, respectively.

Kinetic measurements. We used an Applied Photophysics (Surrey, UK) DX-17MV single-mixing stopped-flow microvolume spectrophotometer. Intrinsic Trp emission was monitored using 295 nm excitation light. Both slits of the excitation monochromator were set in 4 nm. The emitted fluorescence was collected between 300 and 400 nm, using a glass filter and a XF1001-330W880 filter from Omegafilters (Brattleboro, USA). The photomultiplier voltage was 700 V. Thousand data points were collected for each shot. The split time-base feature of the instrument was used to collect more data points at the beginning of the reaction (up to 5 s). At least three and up to five shots were averaged in each experiment using 100 μL of each reactant per shot in 1:1 mixing mode. The dead-time of the instrument is 4 ms.

Data analysis. The three curves produced with the different setups (see below) were fitted simultaneously by performing a Monte Carlo simulated annealing, where the cost function minimized was the square root of the quadratic difference between calculated points and experimental ones.

Results and discussion

We used a stopped-flow fluorometer to study the kinetics of membrane binding and conformational changes associated with binding of L-BABP. We measured the time dependence of fluorescence intensity of the single Trp of L-BABP in three different experimental set-ups: System I, native protein was mixed with anionic lipid membranes; System II, native protein in a solution containing the soluble quencher of fluorescence acrylamide was mixed with anionic lipid membranes prepared in a buffer containing the same concentration of soluble quencher; System III, native protein was mixed with anionic lipid membranes containing 5% of dioleoylphosphoethanolamine-nitrobenzoxadiazol (NBD-PE). Fluorescence intensity of Trp6 in system I is sensitive both to the process of membrane binding and to protein conformational change as described below. The fluorescence intensity in the system II contains information about the degree of exposure of Trp6 to the aqueous environment. This exposure depends on the extent of unfolding of the protein and on the level of penetration into the lipid membrane of the segment containing the Trp6 residue. Fluorescence changes in system III are mainly influenced by the resonance energy transfer between Trp6 and the nitrobenzoxadiazol group in NBD-PE, and can be considered as a measure of protein binding independently of the protein conformational state. In control experiments we made the same measurements using vesicles prepared with the zwitterionic lipid POPC and POPC with 5% NBD-PE. L-BABP does not bind to these membranes [2]. In these controls, we observed no time-dependent fluorescence changes after mixing the native protein with lipid vesicles in stopped-flow experiments.

Steady-state measurements

To understand the time evolution of the fluorescence intensity we first studied the steady-state fluorescence spectra at equilibrium. Both for stopped-flow and steady-state experiments we selected lipid, protein and salt concentrations at which the equilibrium of binding is largely shifted to the membrane-bound form of the protein ([2] and control experiments not shown here). We measured the area between 300 and 400 nm of the fluorescence emission spectra, corresponding to the band pass of the optical filters used in the emission channel of the stopped flow equipment. When L-BABP was bound to POPG membranes, corresponding to kinetic experiment in system I, the spectrum was red-shifted the area was larger than for the free protein in solution. We have not studied the origin of this effect, but it can be proposed that it was due both to de-quenching of Trp6 fluorescence and to changes in the dielectric and dynamic properties of the environment surrounding Trp6. Met107 is near to Trp6 in the native structure. The distance between the sulfur atom and the plane of the indole ring is 4.5 Å [6]. Met107 is probably attenuating the fluorescence of Trp6 in the native structure [7]. The average distance between these residues should increase in an unfolded or partly unfolded state, producing an increase in the fluorescence intensity of Trp6. Also, the change in the dielectric constant of Trp6 environment, when the native protein moves from the aqueous solution to the membrane interface, could have influence on the fluorescence intensity.

To understand the behaviour of system II we measured the Stern–Volmer constant for the quenching with acrylamide. This quenching depends on the exposure of the indole group to the aqueous environment. Fluorescence steady-state measurements yielded Stern–Volmer constants (K_{sv}) 2.09 and 2.00 M^{-1} for the native protein in solution and partly unfolded membrane-bound protein, respectively. L-BABP can acquire partly unfolded conformations in acidic solutions [3]. The Stern–Volmer constant for the quenching with acrylamide in these species was $K_{sv} = 10\ M^{-1}$. Considering that L-BABP is partly unfolded in the interface, the absence of an increased quenching in the membrane-bound protein indicated that Trp6 was buried to some extent into the membrane, in agreement with the results of our Molecular Dynamic simulations [8].

Binding of L-BABP to the anionic lipid membrane containing 5% of NBD-PE, corresponding to the kinetic experiment in system III, produced a decrease of 16% in the fluorescence intensity as compared to the protein in solution, and of 26% related to the protein bound to the anionic membrane in the absence of NBD. Quenching of Trp6 fluorescence occurred together with the increase in the fluorescence emission of NBD at 530 nm (not shown) indicating that the quenching of Trp6 fluorescence was due to the resonance energy transfer process [9]. No quenching by energy transfer was observed when L-BABP was not bound to the membrane, which is in the presence of zwitterionic lipid membranes containing 5% NBD-PE. We calculated a Förster distance Ro = 1 nm for the couple indole-NBD [10]. Considering this value, the efficiency of energy transfer that we measured is in agreement with a localization of the indole within the plane of NBD probes in the lipid head group [11].

Please cite this article in press as: V. Galassi et al., Kinetics of lipid-membrane binding and conformational change of L-BABP, Biochem. Biophys. Res. Commun. (2009), doi:10.1016/j.bbrc.2009.03.103

Differential detection of protein binding and unfolding. Kinetics measurements

To discriminate between the processes of binding and unfolding we compared the time dependence of the fluorescence intensity in the three systems. As a general case, we can postulate the existence of several states of L-BABP with different contribution to the fluorescence intensity. The time dependence of fluorescence intensity after mixing in the system I can be expressed as:

$$F_o(t) = \sum_i \overline{F}^i_o [P_i](t) \quad (1)$$

$[P_i](t)$ are the concentrations of protein in the states i, $\overline{F}^i_o$ coefficients are the fluorescence intensities of the sample when the whole amount of protein is in the state i. If the mixture is made in the presence of a concentration [Q] of soluble quencher (system II), the coefficients $\overline{F}^i_o$ are decreased by a factor $1/(1 + K^i_{SV}[Q])$, where K^i_{SV} are the Stern–Volmer constant for the protein in the state i. The time dependence of the fluorescence intensity in this case is:

$$F_{SV}(t) = \sum_i \frac{\overline{F}^i_o}{1 + K^i_{SV}[Q]} [P_i](t) = \sum_i \overline{F}^i_{SV} [P_i](t) \quad (2)$$

When L-BABP binds to lipid membranes containing NBD-PE (system III), the time dependence of fluorescence is described by

$$F_{ET}(t) = \sum_i \frac{\overline{F}^i_o}{K^i_{ET}} [P_i](t) = \sum_i \overline{F}^i_{ET} [P_i](t) \quad (3)$$

where K^i_{ET} are factors that take into account the decrease in fluorescence intensity due to energy transfer to NBD.

After mixing the protein with anionic lipid membranes (system I, Fig. 1A) the fluorescence increased in a way that can not be described with a single exponential, indicating the existence of a multistep process. This single curve can not reveal which is the process that takes place after mixing. The increase in fluorescence can reflect both a change of environment due to the translocation to the membrane of a native protein and a de-quenching due to a local unfolding process. This increase occurs simultaneously with the binding to the interface (see below, system III). The same mixing experiment, but in the presence of a soluble quencher, system II, was of major importance to understand the binding-conformational change mechanism: Fig. 1B shows a lag time of about 5–10 s in which the fluorescence was not increasing. Within this time span, an *increase* in the fluorescence intensity was observed in the absence of acrylamide (Fig. 1A), and the fluorescence was quenched by the probe anchored to the membrane (system III Fig. 1C). Therefore, we concluded that L-BABP increased the exposure of Trp6 to the aqueous environment at the same time that it was bound to the membrane. The compensation of the fluorescence changes due to these processes resulted in a steady value of fluorescence during the first portion of the curve in Fig. 1B. After the lag-time, the fluorescence intensity in system II increased, indicating that the Trp6 was removed from the contact with the aqueous medium. We propose that this shielding is due to partial or total burial of the residue into the lipid membrane. Mixing of L-BABP with anionic lipid membranes containing 5% of NBD-PE produced a decrease in the fluorescence intensity as shown in Fig. 1C. Because the energy transfer depends only on the distance between the donor and the plane of acceptors, we can associate this decrease with the binding process and location within the lipid polar head group independently of the protein conformation. These observations led us to propose the existence of two locations in the interface for an unfolded or partly unfolded state, U, according to the following kinetic model:

$$N_s \xrightarrow{k_1} U_{\text{int}} \xrightarrow{k_2} U_{\text{memb}}$$

N_s is the native protein in the aqueous phase, U_{int} is a partly unfolded protein located in the interface, within the lipid polar head group region, in a place in which the protein is still in contact with the aqueous face. The existence of this state, populated during the first 5–10 s, is revealed by the observation that the protein was bound to the interface according to Fig. 1C and had an increased accessibility to acrylamide, as depicted in Fig. 1B and D. U_{memb} is a partly unfolded state in which Trp6 is further penetrating into the polar head group region, segregating Trp6 from the contact with the aqueous medium. This state is evidenced by the increase in fluorescence intensity in system II, after a lag time of about 5–10 s.

The solutions of the differential equations for this model are [12]:

$$[N_s](t) = [N_s]_0 e^{-k_1 t} \quad (4)$$

$$[U_{\text{int}}](t) = [N_s]_0 \frac{k_1}{k_2 - k_1} (e^{-k_1 t} - e^{-k_2 t}) \quad (5)$$

$$[U_{\text{memb}}](t) = [N_s]_0 \left\{ 1 - \frac{(k_2 e^{-k_1 t} - k_1 e^{-k_2 t})}{k_2 - k_1} \right\} \quad (6)$$

To fit the experimental curves, we introduced these time-dependent concentrations in (1)–(3). For system I, the resulting equation is

$$F_o(t) = \overline{F}^{NS}_o [N_s]_0 e^{-k_1 t} + \overline{F}^{UI}_o [N_s]_0 \frac{k_1}{k_2 - k_1} (e^{-k_1 t} - e^{-k_2 t}) + \overline{F}^{UM}_o [N_s]_0 \left\{ 1 - \frac{(k_2 e^{-k_1 t} - k_1 e^{-k_2 t})}{k_2 - k_1} \right\} + f_{sc} \quad (7)$$

where $[N_s]_0$ is the analytical concentration of the protein. $\overline{F}^{NS}_o$, $\overline{F}^{UI}_o$ and $\overline{F}^{UM}_o$ are the fluorescence coefficients of the three species contributing to the mechanism. f_{sc} is the contribution from scattered light.

The resulting equation to fit the curve corresponding to system II was

$$F_{SV}(t) = \frac{\overline{F}^{NS}_o}{1 + K^{NS}_{SV}[Q]} [N_s]_0 e^{-k_1 t} + \frac{\overline{F}^{UI}_o}{1 + K^{UI}_{SV}[Q]} [N_s]_0 \frac{k_1}{k_2 - k_1} (e^{-k_1 t} - e^{-k_2 t}) + \frac{\overline{F}^{UM}_o}{1 + K^{UM}_{SV}[Q]} [N_s]_0 \left\{ 1 - \frac{(k_2 e^{-k_1 t} - k_1 e^{-k_2 t})}{k_2 - k_1} \right\} + f_{sc} \quad (8)$$

where [Q] is the concentration of soluble quencher. K^{NS}_{SV}, K^{UI}_{SV}, and K^{UM}_{SV} are the Stern–Volmer constants for the three proposed species. It must be noted that if the different states of the protein had the same degree of exposure to the aqueous solvent, that is the same values of K_{SV}, the terms containing the Stern–Volmer constants would factor out of the summation in Eq. (2) and the ratio between the curves described by Eqs. (1) and (2) should be constant as a function of time. On the other hand, if the different states had different exposure to the aqueous environment, a time-dependent value of $F_o(t)/F_{SV}(t)$ would be expected along with time-dependent changes in the populations of states. This is clearly the case as can be observed in the ratio between these curves shown in Fig. 1D. Measurements made with system III were fitted according to

$$F_{ET} = \frac{\overline{F}^{NS}_o}{K^{NS}_{ET}} [N_s]_0 e^{-k_1 t} + \frac{\overline{F}^{UI}_o}{K^{UI}_{ET}} [N_s]_0 \frac{k_1}{k_2 - k_1} (e^{-k_1 t} - e^{-k_2 t}) + \frac{\overline{F}^{UM}_o}{K^{UM}_{ET}} + [N_s]_0 \left\{ 1 - \frac{(k_2 e^{-k_1 t} - k_1 e^{-k_2 t})}{k_2 - k_1} \right\} + f_{sc} \quad (9)$$

In this system, the traces of the stopped-flow experiment showed an irreproducible dependence with the time after 30 s. We have no explanation for this behaviour and decided to use only the reproducible part of the curves in system III, that is up to 22 s. The intensities were corrected for the inner filter effect due to NBD.

The curves obtained with the three set-ups were fitted simultaneously using Eqs. (7)–(9) (see Materials and methods). The values

Please cite this article in press as: V. Galassi et al., Kinetics of lipid-membrane binding and conformational change of L-BABP, Biochem. Biophys. Res. Commun. (2009), doi:10.1016/j.bbrc.2009.03.103

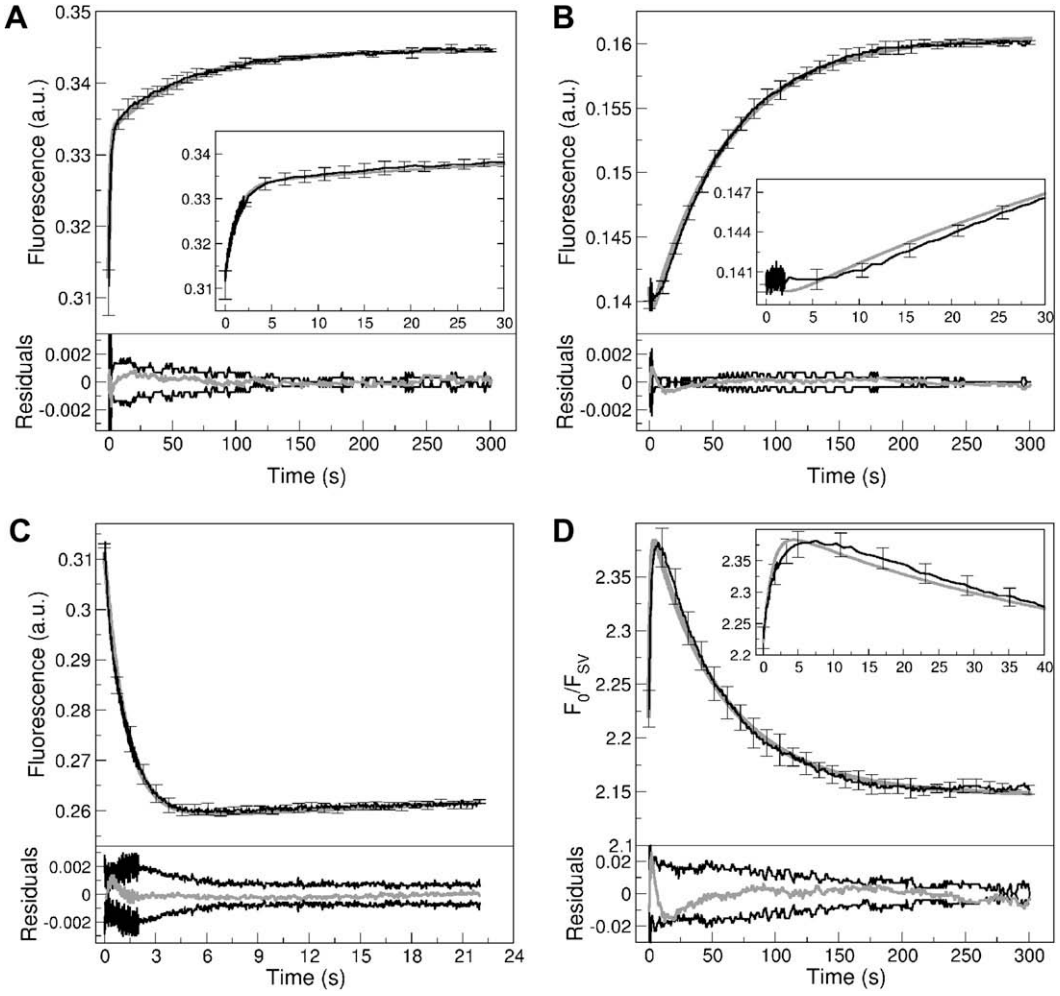

Fig. 1. Florescence of Trp6 in L-BABP as a function of time after mixing with SUVs. (A) Pure L-BABP was mixed with POPG LUVs. (B) L-BABP in the presence of 0.545 M acrylamide was mixed wit POPG LUVs in the presence of 0.545 M acrylamide. (C) Pure L-BABP was mixed with POPG LUVs containing 5% of NBD-PE. (D) The ratio between the curves in A and B. Concentrations in the cell after mixing were 1 mM lipid and 10 μM protein. Dark traces are the experimental results. Grey traces are the curves resulting from the fitting process. Error bars are the standard deviation of the experimental data. The insets in panels A, B, and D are the amplification of the first portion of the corresponding curves. *Residuals:* grey lines are the differences between the simulated and the experimental curves, black lines are the range of the experimental error.

of $\overline{F}_o^{NS}$, $\overline{F}_o^{UM}$, K_{SV}^{NS}, K_{SV}^{UM}, K_{ET}^{NS}, K_{ET}^{UM}, and f_{sc} were measured experimentally and used as initial values. They were allowed to vary within a restricted range around the experimentally measured values in the fitting procedure. The values reached at convergence are shown in Table 1. As a result of the fitting process we obtained the spectroscopic parameters that characterize the intermediate state U_{int} (Table 1), and the values of the kinetic constants: $k_1 = (0.80 \pm 0.05)\ \text{s}^{-1}$ and $k_2 = (0.017 \pm 0.001)\ \text{s}^{-1}$. The value obtained for the intrinsic fluorescence of U_{int} was larger than for the native protein in solution, N_s, and similar to the bound protein in the final state U_{memb}. Probably, this effect was due to the release of Trp6 fluorescence quenching by Met107. The Stern–Volmer constant for the intermediate in the interface, U_{int}, indicates that Trp6 is more exposed to the aqueous medium than in the native protein in solution and in the final U_{memb} state. As expected, Trp6 in U_{int} is less exposed to the aqueous medium than in the acidic, partly unfolded states in solution. Finally, the fitting procedure produced the same values of K_{ET} for U_{int} and U_{memb}, suggesting that subtle differences in location of these states can not be discriminated by NBD anchored to the membrane. The overall good quality of the curve fitting, including the capacity to reproduce the lag in the increase of fluorescence intensity in system II, strongly support the mechanism proposed.

Table 1
Intrinsic fluorescence intensities, $\overline{F}_i$, Stern–Volmer quenching constants, K_{SV}^i, and fluorescence attenuation factors due to energy transfer, K_{ET}^i, for the native protein in dolution, N_s, partly unfolded state in the interface, U_{int}, and in the membrane U_{memb}.

	N_s	U_{int}	U_{memb}
$\overline{F}_0^i$ ($\times 10^{-5}$ a.u.)	0.243 ± 0.003	0.264 ± 0.003	0.270 ± 0.005
K_{SV}^i (M^{-1})	1.96 ± 0.04	2.40 ± 0.07	1.87 ± 0.05
K_{ET}^i	1	1.37 ± 0.02	1.35 ± 0.04

We conclude that L-BABP binds to anionic lipid membranes in a single fast step simultaneously with a conformational change that leads the protein to a partly unfolded state located in the membrane interface. Both processes, binding and conformational change, can be driven by electrostatic forces according to previous results [2,8]. In a second slower step, Trp6 is shielded from the contact with the water solvent, probably due to further penetration within the polar head group region. Our Molecular Dynamics simulations show that penetration of L-BABP within the polar head group region occurs with release of water molecules from contact with the protein and the lipid head group [8]. It can be proposed that this dehydration process contributes to the energetic barrier between the species U_{int} and the further penetrated U_{memb}.

Please cite this article in press as: V. Galassi et al., Kinetics of lipid-membrane binding and conformational change of L-BABP, Biochem. Biophys. Res. Commun. (2009), doi:10.1016/j.bbrc.2009.03.103

Acknowledgments

This work was supported by grants from CONICET, SECyT-UNC and FONCyT. The Biocrystallography laboratory of the University of Verona is funded by a grant from the Italian Ministry of Education and Scientific Research. We are indebted to Dr. Rita H. de Rossi, Dept. Organic Chemistry, FCQ, UNC, for allowing us to use the stopped flow facility.

References

[1] S.H. White, W.C. Wimley, Membrane protein folding and stability: physical principles, Annu. Rev. Biophys. Biomol. Struct. 28 (1999) 319–365.
[2] V. Nolan, M. Perduca, H.L. Monaco, B. Maggio, G.G. Montich, Interactions of chicken liver basic fatty acid binding-protein with lipid membranes, Biochim. Biophys. Act. 1611 (2003) 98–106.
[3] V. Nolan, M. Parduca, H.L. Monaco, G.G. Montich, Chicken liver bile acid-binding protein is in a compact partly folded state at acidic pH. Its relevance to the interaction with lipid membranes, Biochemistry 44 (2005) 8486–8493.
[4] G. Scapin, P. Spadon, M. Mammi, G. Zanotti, H.L. Monaco, Crystal structure of chicken liver basic fatty acid-binding protein at 2.7 Å resolution, Mol. Cell Biochem. 98 (1990) 95–99.
[5] M.J. Hope, M.B. Bally, G. Webb, P.R. Cullis, Production of large unilamellar vesicles by a rapid extrusion procedure. Characterization of size distribution, trapped volume and ability to maintain a membrane potential, Biochim. Biophys. Acta 812 (1985) 55–65.
[6] D. Nichesola, M. Perduca, S. Capaldi, M.E. Carrizo, P.G. Righetti, H.L. Monaco, Crystal structure of chicken liver basic fatty-acid binding protein complexed with cholic acid, Biochemistry 43 (2004) 14072–14079.
[7] T. Yuan, A.M. Weljie, H.J. Vogel, Tryptophan fluorescence quenching by methionine and selenomethionine residues of calmodulin: orientation of peptide and protein binding, Biochemistry 37 (1998) 3187–3195.
[8] M.A. Villarreal, M. Perduca, H.L. Monaco, G.G. Montich, Binding and interactions of L-BABP to lipid membranes studied by molecular dynamic simulations, Biochim. Biophys. Acta 1778 (2008) 1390–1397.
[9] T. Förster, Experimentelle und theoretische Untersuchung des zwischenmolekularen Übergangs von Elecktronenanregungsenergie, Zeitschrift für Naturforschung 4a (1949) 321–327.
[10] J.M. Dixon, M. Taniguchi, J.S. Lindsey, PhotochemCAD 2. A refined program with accompanying spectral databases for photochemical calculations, Photochem. Photobiol. 81 (2005) 212–213.
[11] P.K. Wolber, B.S. Hudson, An analytic solution to the Förster energy transfer problem in two dimensions, Biophys. J. 28 (1979) 197–210.
[12] F. Ruff, I.G. Csizmadia, Organic Reactions. Equilibria, Kinetics and Mechanism, Elsevier, 1994.

Please cite this article in press as: V. Galassi et al., Kinetics of lipid-membrane binding and conformational change of L-BABP, Biochem. Biophys. Res. Commun. (2009), doi:10.1016/j.bbrc.2009.03.103